

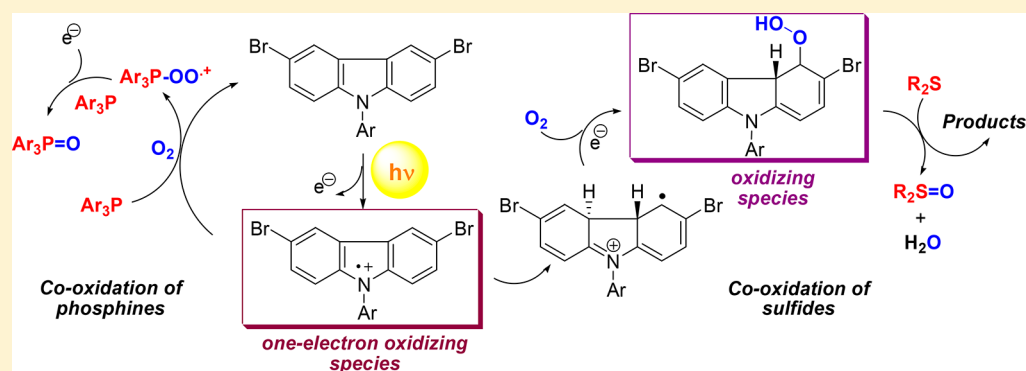
Photochemical Co-Oxidation of Sulfides and Phosphines with Tris(*p*-bromophenyl)amine. A Mechanistic Study

Sergio M. Bonesi,^{*,†,‡} Stefano Protti,[‡] and Angelo Albini[‡]

[†]Departamento de Química Orgánica, CIHIDECAR-CONICET, 3^{er} Piso, Pabellón 2, Ciudad Universitaria, FCEyN, University of Buenos Aires, Buenos Aires 1428, Argentina

[‡]PhotoGreen Lab, Department of Chemistry, University of Pavia, V. leTaramelli 12, 27100 Pavia, Italy

S Supporting Information

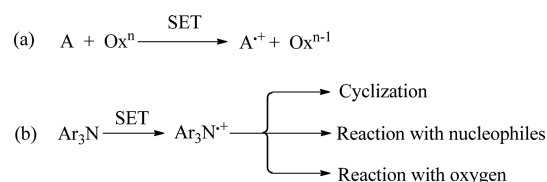


ABSTRACT: The photochemistry of tris(*p*-bromophenyl)amine was investigated in a nitrogen- and oxygen-flushed solution under laser flash photolysis conditions. The detected intermediates were the corresponding amine radical cation (“Magic Blue”) and the *N*-phenyl-4a,4b-dihydrocarbazole radical cation that, under an oxygen atmosphere, is converted to the corresponding hydroperoxyl radical. The role of the last species was supported by the smooth co-oxidation of sulfides to sulfoxides. On the other hand, co-oxidation of nucleophilic triarylphosphines to triarylphosphine oxides arose from an electron transfer between the photogenerated “Magic Blue” and phosphine that prevented the amine cyclization. In this case, intermediate $\text{Ar}_3\text{POO}^{\bullet+}$ was found to play a key role in phosphine oxide formation.

INTRODUCTION

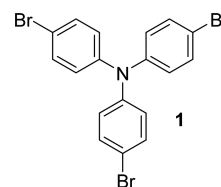
Single-electron-transfer processes [SETs (Scheme 1a)] play a key role in fields ranging from synthetic chemistry¹ to material

Scheme 1. (a) Single-Electron-Transfer (SET) Processes and (b) SET Occurring on Triaryl Amines and Following the Observed Pathways



chemistry.² However, because the key intermediate contains an unpaired electron, it is much more reactive than the starting compound, and therefore multielectron processes, interference with oxygen, and chain reactions often followed spontaneously SET. In the case of SET-based oxidation processes, organic oxidants, such as the popular “Magic Blue”,³ are often preferred over metal ions for mechanistic investigations because these reagents allow better control of the kinetics of the reaction. In this context, the case of tris(4-bromophenyl)amine [1 (Chart 1)], the precursor

Chart 1. Structure of Tris(4-bromophenyl)amine



of Magic Blue would be of high interest, because in the past, structurally related but less oxidizing reagents such as di- and triaryl amines were reported to undergo smooth cyclization to the corresponding carbazoles upon irradiation. The reactions of such compounds in the presence of nucleophiles under photochemical conditions have also been investigated in detail,³ and the competition between different processes may be more informative. Furthermore, the photoinduced electrocyclization of stable triarylamine radical cations has been thoroughly described by Fox and co-workers.⁴

Received: April 11, 2018

Published: May 25, 2018

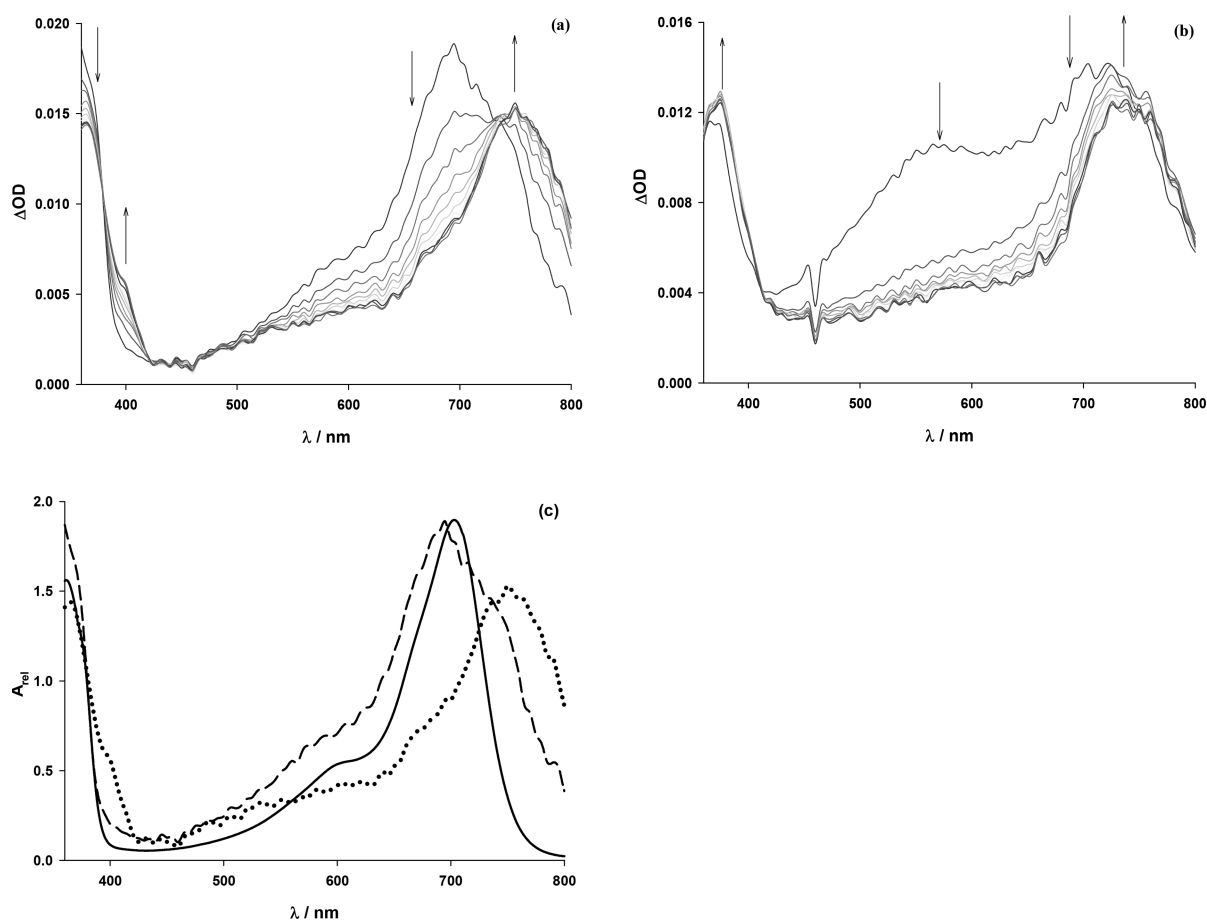


Figure 1. Time-resolved absorption spectra of transients of tris(*p*-bromophenyl)amine (**1**, 0.3 mM) recorded 200 μs after the laser pulse (355 nm) in MeCN under (a) nitrogen and (b) oxygen atmospheres. (c) Absorption spectra of commercial Magic Blue (—), photogenerated $1^{\bullet+}$ recorded 10 μs after the pulse (---), and transient 2 recorded 90 μs after the pulse (···).

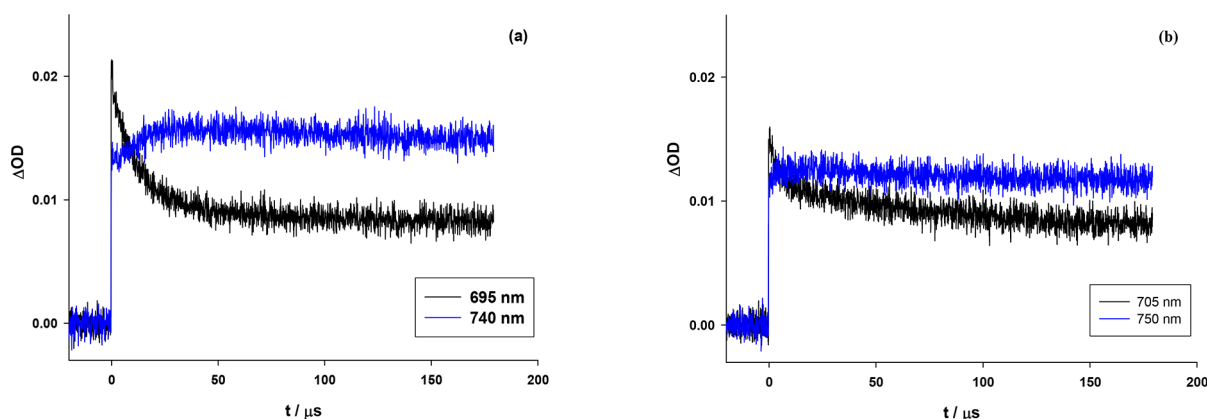


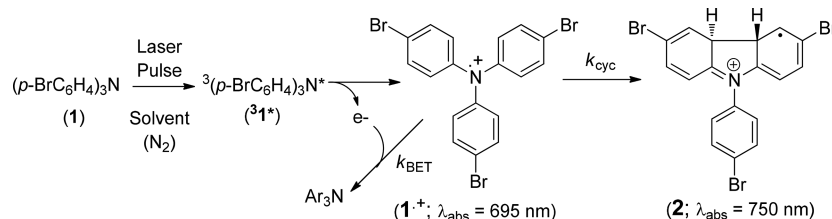
Figure 2. Decay traces of transients from tris(*p*-bromophenyl)amine (0.3 mM) recorded after the laser pulse (355 nm) in MeCN under (a) nitrogen and (b) oxygen atmospheres.

37 For this purpose, we thought that examining in detail the
38 photochemical behavior of the Magic Blue precursor, viz., tris(*p*-
39 bromophenyl)amine (**1**), in the presence of nucleophilic addi-
40 tives such as sulfides and triarylphosphines, oxygen, and solvents
41 of different nature would be worthwhile.

42 ■ RESULTS

43 **Time-Resolved Spectroscopic Measurements of Tris(*p*-**
44 **bromophenyl)amine (**1**) in Solution.** To obtain mechanistic
45 information about the photochemistry of amine **1** in MeCN at

room temperature, laser flash photolysis studies were performed. 46
Under a nitrogen atmosphere, the initial formation of a transient 47
with three bands centered at 370, 590, and 695 nm was evidenced 48
(see Figure 1). This absorption pattern was identical to that of 49
Magic Blue ($1^{\bullet+}$)⁵ and evolved in 38 μs into a further transient 50
($\lambda_{\text{max}} = 750 \text{ nm}$; $\tau > 200 \mu\text{s}$) that has been assigned, on the basis 51
of previous studies, to dihydrocarbazole **2** (Figure 1).^{4a,6} A com- 52
parison between the absorption spectra of transients $1^{\bullet+}$, **2**, and 53
commercial Magic Blue (Figure 2) pointed out that $1^{\bullet+}$ is formed 54
after the laser pulse. In Figure 2a, the decay of the intermediate 55

Scheme 2. Formation of Transients 1^{*+} and 2 in Nitrogen-Equilibrated Media

56 and its corresponding conversion to 2 are clearly shown, and
57 Scheme 2 depicts the observed stepwise process.

58 On the other hand, in an oxygen-equilibrated solution, the
59 end-of-pulse spectrum showed an additional feature at 550 nm,
60 then evolving to give the same end spectrum as under nitrogen,
61 where the absorption spectra of transients 1^{*+} and 2 were
62 detected (Figure 1b). Figure 2b shows the decay trace of 1^{*+} and
63 the formation trace of transient 2 recorded after the laser pulse
64 under an oxygen atmosphere. The quantum yield values for for-
65 mation of the two intermediates along with their lifetime were
66 measured under both atmospheres, by using benzophenone in
67 benzene as a reference (Table 1).

Table 1. Measured Quantum Yields (Φ) for the Formation of Intermediates 1^{*+} and 2 under the Examined Conditions^a

transient	λ_{abs} (nm)	atmosphere	concentration (M)	ϕ	τ (μs)
1^{*+}	695	N_2	1.24×10^{-6}	0.158	39
		O_2	8.29×10^{-7}	0.077	
2	750	N_2	3.53×10^{-7}	0.066	>200
		O_2	2.17×10^{-7}	0.030	

^aMeasured in MeCN after the laser pulse (355 nm); $\epsilon(1^{*+}) = 19000 \text{ M}^{-1} \text{ s}^{-1}$, and $\epsilon(2) = 30000 \text{ M}^{-1} \text{ s}^{-1}$. The initial absorbance of 1 was fixed at 0.40. Actinometer: solution of benzophenone in benzene under a N_2 atmosphere [$A(355 \text{ nm}) = 0.37$]; $\epsilon(\text{ketyl radical}) = 7220 \text{ M}^{-1} \text{ cm}^{-1}$.

68 The fleeting band located at 550 nm in the time-resolved
69 absorption spectrum of tris(*p*-bromophenyl)amine 1 (see Figure 1b)
70 was assigned to the charge-separated complex between 1 and
71 molecular oxygen that is an energetically favorable process in
72 polar solvents as it was proposed by Wilkinson⁷ and in a recently
73 reported study.⁸ Scheme 3 shows the formation of the charge-
74 transfer complex that is converted to the tris(*p*-bromophenyl)-
75 amine radical cation (1^{*+}) and superoxide ion, and Figure 3
76 depicts the decay trace of the charge-transfer complex in MeCN
77 under an O_2 atmosphere.

78 The charge-transfer complex trace shown in Figure 3 fitted
79 with a biexponential decay and two half-lifetime decays were

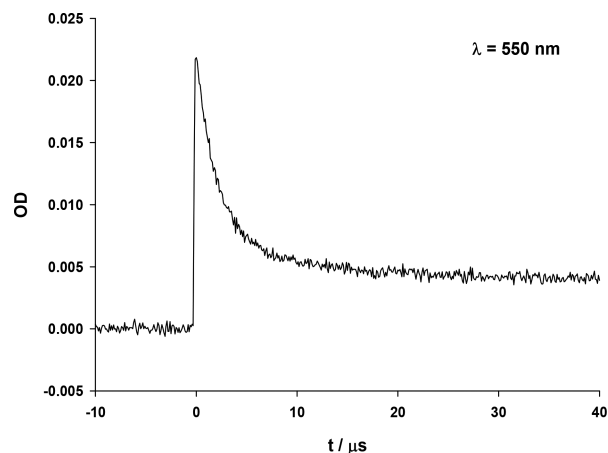
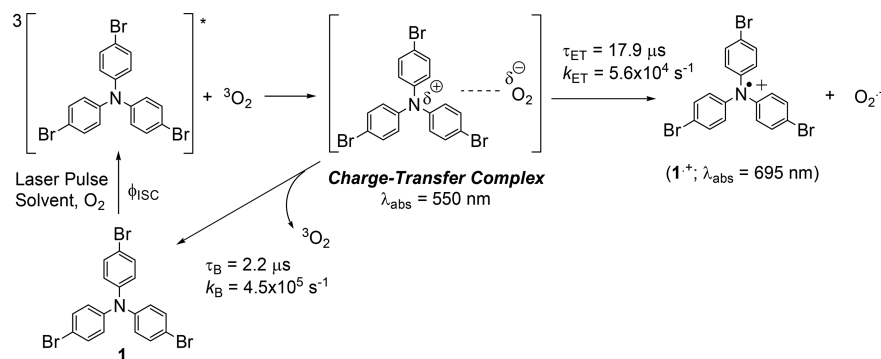


Figure 3. Decay trace of the charge-transfer complex recorded at 550 nm after excitation with a laser pulse (355 nm) of a solution of tris(*p*-bromophenyl)amine (0.3 mM) in MeCN under an oxygen atmosphere.

obtained, viz., 2.2 and 17.9 μs , respectively. The evolution of the
charge-transfer complex involved the reversion pathway to tris(*p*-
bromophenyl)amine (1) and molecular oxygen with a rate constant
 k_B of $4.5 \times 10^5 \text{ s}^{-1}$ and an electron-transfer pathway with a rate
constant k_{ET} of $5.6 \times 10^4 \text{ s}^{-1}$ to provide tris(*p*-bromophenyl)-
amine radical cation (1^{*+}) and superoxide ion (see Scheme 3).

It is noteworthy that under an O_2 atmosphere the quantum
yield values for the formation of 1^{*+} and 2 were halved,
highlighting the interaction between molecular oxygen and 1 in
its triplet excited state to produce singlet oxygen. Therefore, this
competitive pathway diminishes the level of formation of both of
the ensuing intermediates, 1^{*+} and 2 . A similar oxygen effect was
observed during the irradiation of triphenylamine in different
solvents and was attributed to the quenching of the triplet excited
state of triphenylamine by molecular oxygen producing singlet
oxygen with a ϕ_{Δ} of 0.63.⁶ In this case, the corresponding
intermediate dihydrocarbazole, which is equivalent to intermediate 2 ,
is formed to a lesser extent under an oxygen atmosphere than
under a nitrogen atmosphere.

Scheme 3. Formation of a Charge-Transfer Complex and Transient 1^{*+} in Oxygen-Equilibrated Media

99 In addition, the decay traces of transient $\mathbf{1}^{\bullet+}$ at 695 nm were
100 also measured in MeCN after a laser pulse (355 nm) under
101 different conditions (Figure 4) with the aim of determining both

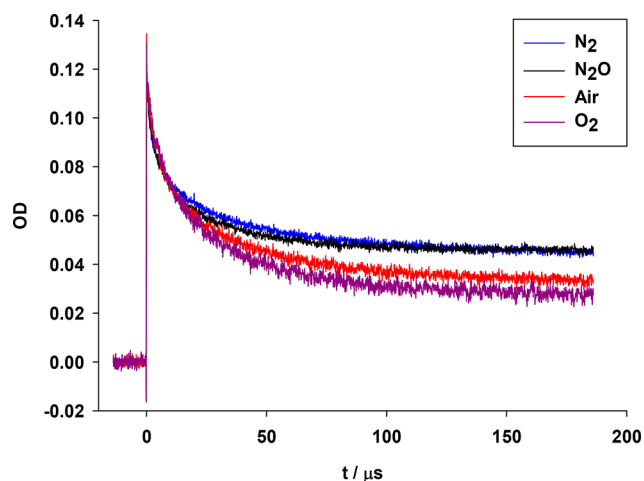


Figure 4. Normalized decay traces of transients from tris(*p*-bromophenyl)amine ($\mathbf{1}$, 0.3 mM) recorded after the laser pulse (355 nm) in MeCN under N_2 (blue), N_2O (black), Air (red), and O_2 (violet) atmospheres.

102 the rate constants of cyclization (k_{cyc}) and back-electron transfer
103 [k_{BET} (see Scheme 2)]. The obtained results are listed in Table 2.

Table 2. Rate Constants, Lifetimes, and Concentrations of Tris(*p*-bromophenyl)amine Radical Cation ($\mathbf{1}^{\bullet+}$) at the End of the Pulse^a

atmosphere	τ_{cyc} (μs)	k_{cyc} (s^{-1})	τ_{BET} (μs)	k_{BET} ($\text{M}^{-1}\text{s}^{-1}$)	concentration (M)
N_2	40.0	2.5×10^4	3.7	2.2×10^{10}	5.93×10^{-6}
N_2O	40.0	2.5×10^4	3.7	2.1×10^{10}	5.93×10^{-6}
air	39.2	2.6×10^4	5.4	1.9×10^{10}	4.39×10^{-6}
O_2	37.0	2.7×10^4	6.4	1.4×10^{10}	3.29×10^{-6}

^aMeasured in MeCN after the laser pulse (266 nm); $\epsilon(\mathbf{1}^{\bullet+}) = 19000 \text{ M}^{-1} \text{ s}^{-1}$. The initial absorbance of the solutions was fixed at 0.64. The error in τ_1 is ± 0.2 and in τ_2 is ± 0.1 .

104 It is noteworthy that the traces of $\mathbf{1}^{\bullet+}$ show a nicely biexponential
105 decay fitting with r^2 values of >0.998 independent of the atmosphere
106 used. As shown in Table 2, τ_{cyc} and k_{cyc} remain almost constant
107 for all the atmospheres used and also in an air-equilibrated
108 solution while a noticeable dependence on the atmosphere was

seen for the back-electron-transfer process (τ_{BET} and k_{BET}), parti- 109
cularly in the cases of air-equilibrated and oxygen atmospheres. 110
Likewise, a similar behavior was observed for the concentration 111
of $\mathbf{1}^{\bullet+}$ at zero time after the laser pulse, which was attributed to 112
the quenching of the triplet excited state of $\mathbf{1}$ by molecular oxygen. 113

Because of the biexponential decay fitting of $\mathbf{1}^{\bullet+}$, the 114
consumption of transient $\mathbf{1}^{\bullet+}$ can be written as eq 1 highlighting 115
the unimolecular electrocyclization step and the bimolecular 116
back-electron-transfer process, where the one ejected electron 117
after the laser pulse is the solvated electron and is designated e^- . 118

$$\frac{d[\mathbf{1}^{\bullet+}]}{dt} = k_{\text{cyc}}[\mathbf{1}^{\bullet+}] + k_{\text{BET}}[\mathbf{1}^{\bullet+}][e^-] \quad (1) \quad 119$$

The conversion of $\mathbf{1}^{\bullet+}$ to $\mathbf{2}$ (see Scheme 2) involves a first- 120
order decay, and the k_{cyc} can be calculated in a straightforward 121
manner from the reciprocal of the half-lifetime (τ_{cyc}^{-1}) under all 122
the conditions examined, and the data thus obtained are listed in 123
Table 2. On the other hand, back electron transfer (BET) of $\mathbf{1}^{\bullet+}$ 124
to tris(*p*-bromophenyl)amine (see Scheme 2 and eq 1) can be 125
represented by k_{BET} . From the slopes of the linear regression of 126
the reciprocal of the concentration of transient $\mathbf{1}^{\bullet+}$ versus time 127
plots, bimolecular rate constants, k_{BET} , of $10^{10} \text{ M}^{-1} \text{ s}^{-1}$ were 128
obtained under all the conditions examined (see Table 2). 129

Co-Oxidation of Sulfides and Phosphines. The oxidation 130
activity of the photogenerated intermediates, namely, $\mathbf{1}^{\bullet+}$ and $\mathbf{2}$, 131
was tested by irradiating solutions of $\mathbf{1}$ in the presence of some 132
substrates acting as electron donors such as sulfides and phos- 133
phines (see Scheme 4). Under such conditions, $\mathbf{1}$ was consumed 134
while the additives were co-oxidized selectively to the corre- 135
sponding sulfoxides and phosphine oxides. In the case of benzyl 136
ethyl sulfide, however, significant amounts of benzaldehyde were 137
also formed. The results are summarized in Tables 3 and 4. 138

Sulfides (including Ph_2S that is inert toward singlet oxygen⁹) were 139
co-oxidized with a rate ranging from 0.003 and $0.244 \mu\text{mol min}^{-1}$, 140
while the sulfoxidation/electrocyclic cyclization ratio was lower 141
than unity (0.06–0.80) in all of the solvents investigated, the 142
only exception being benzyl ethyl sulfide in a 9/1 MeCN/ H_2O 143
mixture. Nucleophilic triarylphosphines were also co-oxidized with 144
a phosphine oxidation/electrocyclic cyclization ratio ranging 145
from $\sim 26/1$ to $5/1$ under irradiation of amine $\mathbf{1}$ in acetonitrile. 146

Blank experiments were also performed. Thus, irradiation 147
of oxygenated solutions of sulfides and phosphines in all the 148
solvents used in the absence of tris(*p*-bromophenyl)amine 149
($\mathbf{1}$) did not provide any sulfoxides or phosphine oxides. Like- 150
wise, experiments performed under a N_2 atmosphere but in the 151
presence of tris(*p*-bromophenyl)amine ($\mathbf{1}$) did not give any 152
oxide. 153

Scheme 4. Co-Oxidation of Sulfides (top path) and Triarylphosphines (bottom path) in the Presence of $\mathbf{1}$

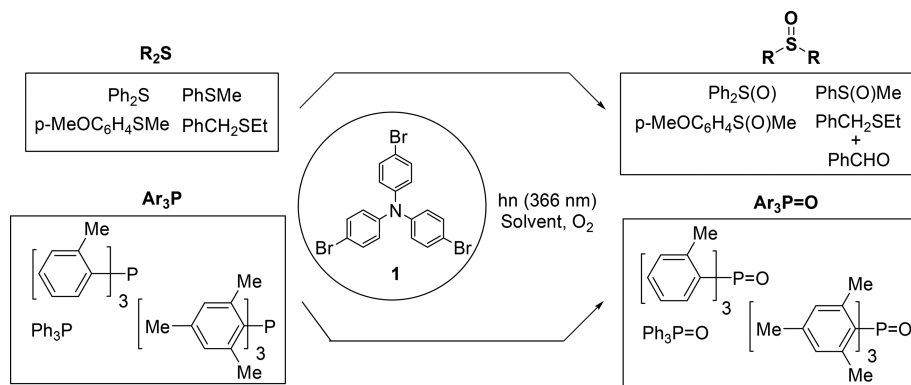


Table 3. Rate of Co-Oxidation of Sulfides upon Irradiation in the Presence of 1^a

substrate	solvent	rate of reaction ($\mu\text{mol min}^{-1}$)		
		sulfoxide	1 ^b	
Ph ₂ S	MeCN	0.003	0.051	
	9/1 MeCN/H ₂ O	0.005	0.041	
	TFE	0.033	0.049	
	DCM	0.008	0.026	
PhSMe	MeCN	0.024	0.20	
	9/1 MeCN/H ₂ O	0.091	0.31	
	TFE	0.193	0.24	
<i>p</i> -MeOC ₆ H ₄ SMe	MeCN	0.026	0.085	
	9/1 MeCN/H ₂ O	0.118	0.239	
	TFE	0.240	0.234	
	DCM	0.005	0.030	
PhCH ₂ SEt	MeCN	0.088	0.065	PhCHO, 0.010
	9/1 MeCN/H ₂ O	0.184	0.150	PhCHO, 0.024
	TFE	0.244	0.320	PhCHO, 0.030
	DCM	0.093	0.024	PhCHO, 0.013

^aA 5×10^{-3} M solution of **1** irradiated in the presence of the chosen sulfide (10^{-2} M) at 310 nm (10×15 W lamps). ^bRate of consumption of **1**.

Table 4. Rate of Co-Oxidation of Triarylphosphines upon Irradiation in the Presence of 1 in MeCN^a

substrate	rate of co-oxidation ($\mu\text{mol min}^{-1}$)	
	phosphine oxide	1 ^b
Ph ₃ P	2.91	0.11
(<i>o</i> -MeC ₆ H ₄) ₃ P	2.75	0.31
(2,4,6-Me ₃ C ₆ H ₂) ₃ P	4.13	0.91

^aA 5×10^{-3} M solution of **1** irradiated in the presence of the chosen phosphine (1.1×10^{-2} M) at 366 nm (high-pressure Hg lamp provided with a 366 nm interference Schott filter). ^bRate of consumption of **1**.

154 Interaction of Sulfides and Triphenylphosphine with

155 **Photogenerated Transients.** Time-resolved spectroscopy
156 was applied to solutions of **1** in the presence of selected sulfides
157 and triphenylphosphine. Diphenyl sulfide, thioanisole, and benzyl
158 ethyl sulfide caused no change in the previously observed transients.
159 On the other hand, *p*-methoxythioanisole and triphenylphosphine
160 quenched radical cation **1**^{•+} as shown in Figure 5.

161 In the case of *p*-methoxythioanisole and triphenylphosphine,
162 the observed first-order decay constant (k_{obs}) of **1**^{•+} depends
163 linearly on the quencher concentration as shown in eq 2.

$$164 \quad k_{\text{obs}} = k_{\text{cyc}} + k_{\text{Q}}[\text{Q}] \quad (2)$$

165 Plotting k_{obs} versus quencher concentration [Q] resulted in a
166 linear correlation (see Figure 5). The corresponding bimolecular
167 rate constants were obtained from the slope of the linear regres-
168 sions, viz., $k_{p\text{MeO}} = 9.7 \times 10^5 \text{ M}^{-1} \text{ s}^{-1}$ for *p*-methoxythioanisole
169 and $k_{\text{Ph}_3\text{P}} = 2.1 \times 10^6 \text{ M}^{-1} \text{ s}^{-1}$ for triphenylphosphine.

170 ■ DISCUSSION

171 **Analysis of the Intermediates Formed during Irradiation of**
172 **Tris(*p*-bromophenyl)amine (1).** The data presented
173 above show that excitation of **1** with a laser pulse (355 nm)
174 generates two key intermediates in both N₂- and O₂-saturated
175 solutions. However, one of these species reacts efficiently with
176 molecular oxygen, as shown in Scheme 5. Photoionization of **1**

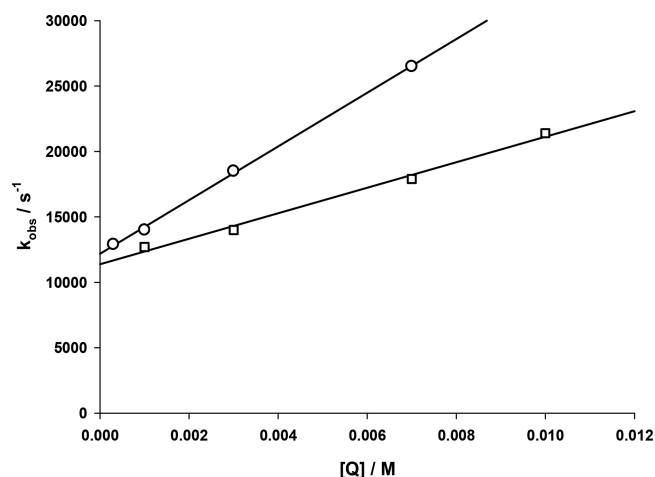


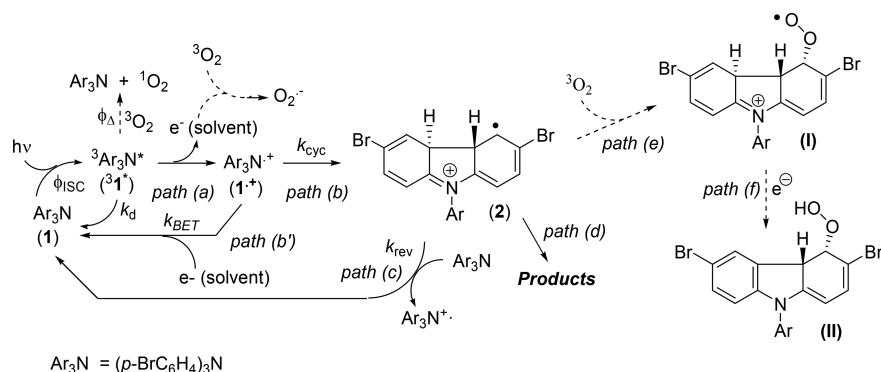
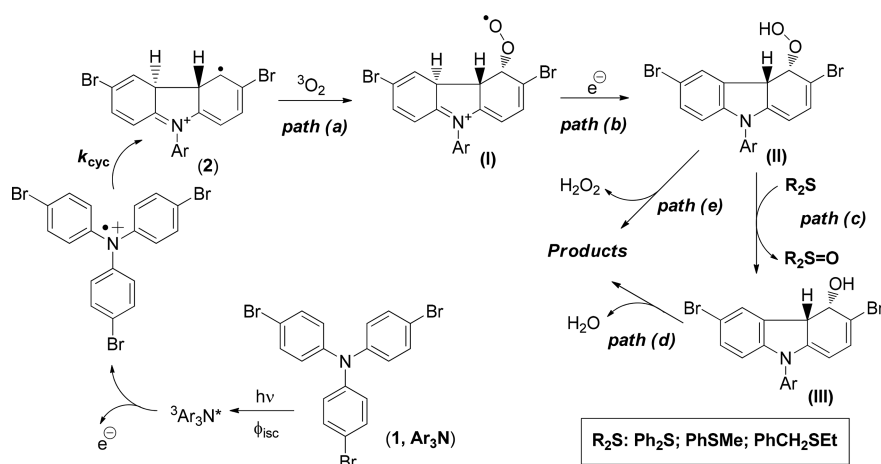
Figure 5. Quenching of **1**^{•+} with increasing concentrations of *p*-methoxythioanisole (□) and triphenylphosphine (○). Straight lines are the best linear regression fits.

forms radical cation **1**^{•+} (path a). Under a nitrogen atmosphere, 177
electrocyclization to radical cation **2** occurs [$k_{\text{cyc}} = 2.5 \times 10^4 \text{ s}^{-1}$ 178
in acetonitrile (path b)] in competition with electron recom- 179
bination [$k_{\text{BET}} = 2.2 \times 10^{10} \text{ M}^{-1} \text{ s}^{-1}$ in acetonitrile (path b')]. Via 180
an ensuing an electron-transfer pathway (path c) intermediate, **2** 181
reverts to amine **1** in competition with formation of products 182
(path d). Irradiation of di(tri)arylamines can be counted among 183
the many mild conversions into carbazoles.^{6,10,11} Indeed, the 184
photochemical preparation of carbazoles under visible light in the 185
presence of a copper-based sensitizer has been reported,⁷ and 186
formation of the triarylamine radical cation followed by cycliza- 187
tion to the dihydrocarbazole intermediate that in turn provides a 188
substituted carbazole was also proposed.^{11f} However, when amine 189
1 was irradiated under visible light photoredox catalysis conditions, 190
no tribromocarbazole was observed, and only *N*-phenylcarbazole 191
was obtained in a low yield (>16%).^{11f} 192

On the other hand, under aerobic conditions, amine **1** in its 193
triplet excited state sensitizes singlet oxygen, thus halving the 194
formation of intermediates **1**^{•+} and, as a consequence, **2**, as can be 195
judged from the quantum yields obtained under an oxygen atmo- 196
sphere (see Table 1 and compare these values with those obtained 197
under a nitrogen atmosphere). Photoionization of triplet amine (**1**) 198
formed **1**^{•+}, and the ejected electron was trapped, at least in part, 199
by molecular oxygen giving superoxide ion with a bimolecular 200
rate constant of $2 \times 10^{10} \text{ M}^{-1} \text{ s}^{-1}$.¹² Additionally, a back-electron- 201
transfer process (path b' in Scheme 5) can occur between **1**^{•+} and 202
the ejected electron with a bimolecular rate constant (k_{BET}) of 203
 $1.4 \times 10^{10} \text{ M}^{-1} \text{ s}^{-1}$. Cyclization (path b) afforded **2** that reacted 204
with molecular oxygen and provided 4-peroxyl radical (**I**) (path e). 205
Ensuing intramolecular hydrogen atom transfer led to intermediate 206
II (path f), and both intermediates are, at least in part, potential 207
oxidizing agents that are formed during irradiation of amine **1** 208
under an oxygen atmosphere. Superoxide ion then further reacted 209
with adventitious water present in the organic media and led to 210
ROS species, including OH[•], HOO[•], and H₂O₂. 211

Under air-equilibrated conditions, a similar photochemical 212
behavior was observed for **1** in MeCN, where both **1**^{•+} and **2** were 213
detected. Transient **1**^{•+} decays competitively by two pathways, 214
back-electron transfer to amine **1** (path b' in Scheme 4; $k_{\text{BET}} =$ 215
 $1.9 \times 10^{10} \text{ M}^{-1} \text{ s}^{-1}$) and electrocyclization to **2** (path b in Scheme 4; 216
 $k_{\text{cyc}} = 2.6 \times 10^4 \text{ s}^{-1}$). 217

Nitrous oxide is a good quencher of solvated electron and has 218
often been used under pulse radiolysis and laser flash photolysis.¹³ 219

Scheme 5. Proposed Reaction Mechanism of the Photocyclization of **1** (filled arrows, nitrogen atmosphere; dashed arrows, oxygen atmosphere)Scheme 6. Proposed Mechanism for the Co-Oxidation of Sulfides during the Photocyclization of **1**

220 However, bubbling N_2O into a solution of **1** in MeCN had no
 221 effect on the transient intermediates, the competitive rate constants
 222 k_{cyc} and k_{BET} exhibiting the same values under N_2O and N_2
 223 atmospheres (see Table 3). This is due to the fact that chemical
 224 reaction occurs at the geminate pair level ($1^{*\bullet}\cdots e^-$) and no
 225 solvated electron (e^-_{solv}) is formed. Furthermore, comparison of
 226 the rate constant for the reaction of N_2O with the electron ($9 \times$
 227 $10^9 \text{ M}^{-1} \text{ s}^{-1}$)^{13e} and the BET reaction of $1^{*\bullet}$ ($2.1 \times 10^{10} \text{ M}^{-1} \text{ s}^{-1}$)
 228 accounts for the observed spectroscopic behavior.

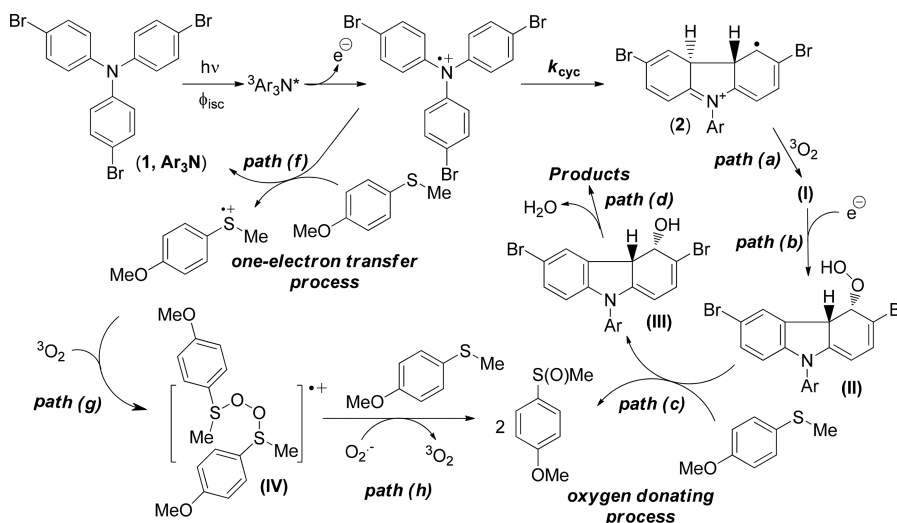
229 With regard to oxygen trapping by **2**, it was surmised that some
 230 intermediates generated during the irradiation may similarly
 231 oxidize other compounds under mild conditions.

232 Photo-Co-Oxidation of Sulfides (Ph_2S , PhSMe , and 233 PhCH_2SEt) in the Tris(*p*-bromophenyl)amine/ O_2 System.

234 In steady-state experiments in which amine **1** was irradiated in
 235 the presence of a range of sulfides, the latter are co-oxidized to
 236 sulfoxides at a rate dependent on their structure and the solvent
 237 used (rate values ranging from 0.003 to $0.244 \mu\text{mol s}^{-1}$) while
 238 amine **1** is consumed efficiently. In addition, the rate ratio of
 239 sulfoxide versus consumption of **1** was <1 (see Table 3), a fact
 240 that we attributed to the intermediacy of one (or more) common
 241 intermediate that is responsible for both cyclization and co-oxidation
 242 of sulfides. It was pointed out that oxidant species such as singlet
 243 oxygen and superoxide ion are formed during the irradiation of
 244 amine **1** under an oxygen atmosphere (see Scheme 6). However,
 245 we can state that the co-oxidation reaction is not a result of a
 246 singlet oxygen reaction as shown by the following evidence:
 247 (1) Sulfones are known to always accompany the sulfoxides in

the singlet oxygen oxidation of sulfides (not observed in that case).
 (2) Benzyl sulfides undergo both sulfoxidation and oxidative
 cleavage to benzaldehyde in protic media,¹⁴ and oxidation also
 takes place on diphenyl sulfides, which are usually nonreactive
 toward singlet oxygen. With regard to superoxide ion, under
 these conditions it is not involved in the co-oxidation of sulfides
 but reduces the radical cation $1^{*\bullet}$ to **1** through a back-electron-
 transfer process. Therefore, according to our results and to the
 literature data, we assigned to hydroperoxide intermediate **II** the
 role of the oxidant species that can transfer an oxygen atom to the
 sulfides to afford the corresponding sulfoxides and a new inter-
 mediate **III**. The latter underwent dehydration to furnish pro-
 ducts (see Scheme 6). Intermediate **II** also underwent aromatization
 by losing hydrogen peroxide, a process that has been previously
 observed to occur at room temperature with a rather slow radical
 chain mechanism.¹⁵ It is worth mentioning that dihydrocarba-
 zole aromatization (path e) and donor oxidation (path c) were
 coupled, and the result depended on the nature of the sulfide.
 Thus, diphenyl sulfide was co-oxidized with an efficiency lower
 than that of thioanisole or benzyl ethyl sulfide as can be observed
 in Table 3.

**Photo-Co-Oxidation of *p*-Methoxythioanisole in the
 Tris(*p*-bromophenyl)amine/ O_2 System.** The photo-co-
 oxidation of *p*-methoxythioanisole with tris(*p*-bromophenyl)-
 amine in the presence of O_2 deserves some comment and addi-
 tional analysis. *p*-Methoxythioanisole sulfoxide could arise from
 two alternative sequences of pathways: (1) an electron-transfer
 process followed by oxidation with molecular oxygen involving

Scheme 7. Proposed Mechanism for the Co-Oxidation of *p*-Methoxythioanisole during the Photocyclization of **1**

276 the sequence from path f to path h (see Scheme 7) and (2)
 277 oxygen donation from intermediate II to *p*-methoxythioanisole
 278 (path c in Scheme 7).

279 The electron-transfer process (path f in Scheme 7) occurs effi-
 280 ciently because tris(*p*-bromophenyl)amine radical cation (**1**^{•+})
 281 has an oxidation potential of 1.16 V versus SCE¹⁶ and can thus
 282 oxidize *p*-methoxythioanisole ($E_{\text{ox}} = 1.13$ V vs SCE),¹⁷ providing
 283 the corresponding radical cation (see Scheme 7). Also, this pro-
 284 cess is a thermodynamically feasible process by -0.03 V. On the
 285 other hand, laser flash spectroscopy showed that *p*-methox-
 286 ythioanisole quenches **1**^{•+} with a bimolecular rate constants $k_{p\text{MeO}}$
 287 $9.7 \times 10^5 \text{ M}^{-1} \text{ s}^{-1}$ (see Figure 4), giving the *p*-methoxythioanisole
 288 radical cation. Once the *p*-methoxythioanisole radical cation
 289 was formed, reaction with molecular oxygen in the presence of
 290 a further molecule of sulfide gave electrophilic radical cation
 291 intermediate IV (path g). Then, this last intermediate reacted
 292 with the sulfide and superoxide ion to give finally two molecules
 293 of the sulfoxides (path h) completing the sequence from path f to
 294 path h.

295 On the other hand, we pointed out above that in the photo-
 296 reaction of tris(*p*-bromophenyl)amine under an O_2 atmosphere,
 297 superoxide ion was also formed (see Scheme 5). A possible
 298 reaction between superoxide ion and sulfide radical cation could
 299 provide a thiodioxirane, an electrophilic intermediate, as pro-
 300 posed by Baciocchi.¹⁸ However, we have earlier demonstrated¹⁹
 301 that dialkyl and diaryl sulfide radical cations react efficiently with
 302 molecular oxygen to give a loose dipolar complex ($\text{R}_2\text{S}-\text{O}-\text{O}^{\bullet+}$)
 303 that further reacts with another molecule of sulfide and gives a
 304 strongly bound electrophilic intermediate ($\text{R}_2\text{S}-\text{O}-\text{O}-\text{SR}_2^{\bullet+}$)
 305 rather than a thiodioxirane intermediate. The strongly bound
 306 electrophilic intermediate was assigned to intermediate IV,
 307 which is shown in Scheme 7. Then, we can conclude that $\text{O}_2^{\bullet-}$
 308 has a role but does not add to the sulfide radical cation. A reason-
 309 able alternative is that superoxide ion operates as an electron
 310 carrier in the reduction of intermediate IV ($\text{ArMeS}-\text{O}-\text{O}-$
 311 $\text{SArMe}^{\bullet+}$) as shown in path h (Scheme 7).

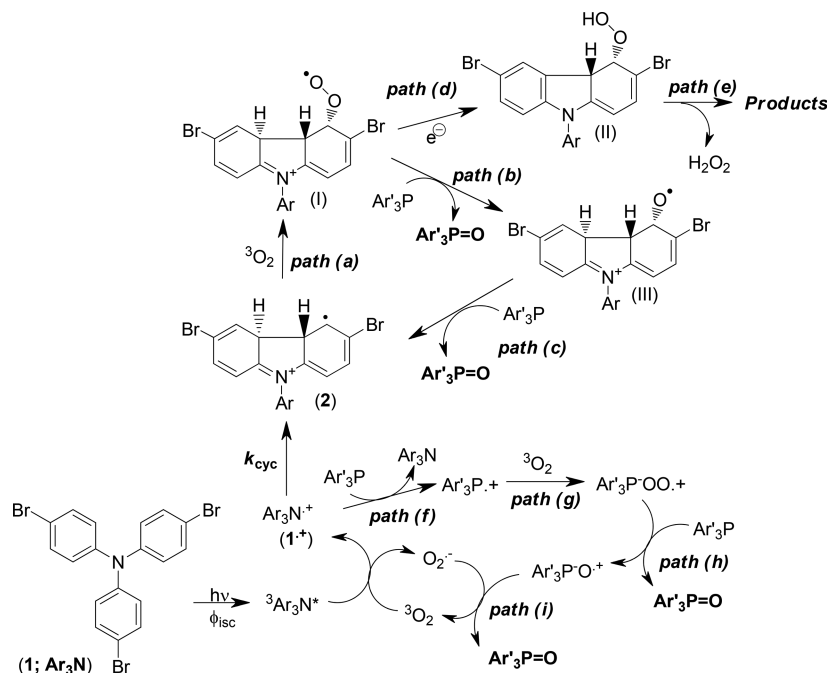
312 It is worth mentioning that the oxygen-donating sequence
 313 pathways illustrated from path a to path d in Scheme 7 providing
 314 *p*-methoxythioanisole sulfoxide cannot be ruled out. In fact, the
 315 cyclization process of tris(*p*-bromophenyl)amine radical cation
 316 (**1**^{•+}) competes to a lesser extent with the one-electron-transfer
 317 process between **1**^{•+} and *p*-methoxythioanisole (path f in Scheme 7).

318 Via comparison of the rate constant values of both competitive
 319 processes ($k_{\text{cyc}} = 2.5 \times 10^4 \text{ s}^{-1}$, and $k_{p\text{MeO}} = 9.7 \times 10^5 \text{ M}^{-1} \text{ s}^{-1}$),
 320 it is clear that the main reaction pathway in the formation of
 321 *p*-methoxythioanisole sulfoxide is the one-electron-transfer
 322 oxidation process (path f) over the cyclization process of the
 323 tris(*p*-bromophenyl)amine radical cation (**1**^{•+}).

324 **Photo-Co-Oxidation of Phosphines.** Phosphines were
 325 stronger oxygen acceptors and, as demonstrated in Table 4 were
 326 co-oxidized efficiently upon irradiation of amine **1** in the pre-
 327 sence of molecular oxygen with a rate ranging from 2.75 to
 328 $4.13 \mu\text{mol s}^{-1}$, while **1** is consumed smoothly. In addition, the rate
 329 ratio of phosphine oxidation versus consumption of **1** increases
 330 from $\sim 5/1$ to $26/1$, indicating that at least two common oxidant
 331 intermediates are responsible for the co-oxidation of phosphines
 332 that inhibit significantly the consumption of amine **1**. On the
 333 basis of steady-state and laser flash photolysis measurements, the
 334 proposed reaction mechanism is shown in Scheme 8.

335 As one can see in Scheme 8, irradiation of **1** gave amine radical
 336 cation **1**^{•+} and superoxide ion. Two competitive pathways exist:
 337 (1) electrocyclization to provide intermediate **2** and (2) one-
 338 electron oxidation of triarylphosphine to furnish the correspond-
 339 ing radical cation. The first path exhibits a rate constant of $2.5 \times$
 340 10^4 s^{-1} , while the second pathway (path f in Scheme 8) exhibits a
 341 rate constant of $2.1 \times 10^6 \text{ M}^{-1} \text{ s}^{-1}$. Following the electrocyclization
 342 pathway, intermediate **2** reacted with molecular oxygen to form **I**
 343 and, after intramolecular hydrogen abstraction, **II**. Both species
 344 are potential oxygen-donating species that are able to transfer
 345 oxygen to the phosphines. It appears to be reasonable that phos-
 346 phines, which are strong nucleophiles, were able to trap inter-
 347 mediate **I** efficiently in competition with intramolecular hydro-
 348 gen abstraction (path b vs path d). Indeed, the reactivity of peroxy
 349 radicals with phosphines has been previously demonstrated.²¹
 350 Thus, **I** oxidized the phosphine to the corresponding phosphine
 351 oxides (path b), P–O bond formation being the driving force for
 352 the process. Finally, intermediate **III** transferred a second oxygen
 353 atom to phosphines (path c), and radical cation **2** was formed.
 354 Thus, two oxygen atoms were sequentially transferred to the
 355 phosphine and led back to **2** completing the oxidation cycle. This
 356 reaction pathway was previously proposed when triphenylamine
 357 was used instead of tris(*p*-bromophenyl)amine.⁶ The oxida-
 358 tion of phosphines inhibits the conversion of intermediate **II**
 359 to products, in agreement with the experimental evidence

Scheme 8. Proposed Mechanism for the Co-Oxidation of Triarylphosphines during the Photocyclization of 1



360 indicating that path b is an efficient process that competes with
361 path d.

362 On the other hand, an alternative oxidation pathway of phosphine
363 may involve the direct one-electron transfer between $1^{\bullet+}$
364 and Ar_3P (path f in Scheme 8) to give triarylphosphine radical
365 cation ($Ar_3P^{\bullet+}$) as it was clearly confirmed by laser flash photolysis
366 experiments and thermodynamic calculations. In fact, triphenyl-
367 phosphine quenched $1^{\bullet+}$ with a bimolecular rate constant (k_{ph_3p})
368 of $2.1 \times 10^6 M^{-1} s^{-1}$ (see Figure 5), and the one-electron-transfer
369 process is thermodynamically feasible ($\Delta G = -0.13 V$), because
370 $1^{\bullet+}$ has an oxidation potential of 1.16 V (vs SCE) whereas the
371 oxidation potential of triphenylphosphine is 1.00 V (vs SCE).²⁰
372 Trapping of generated $Ar_3P^{\bullet+}$ with molecular oxygen occurred,
373 producing peroxy radical cation $Ar_3PO_2^{\bullet+}$ (path g), a reaction
374 pathway that has been previously observed during pulse radio-
375 lysis and laser flash photolysis experiments.²² Reaction of this
376 intermediate with another molecule of Ar_3P and the ensuing
377 mesolytic cleavage yield triarylphosphine oxide and radical cation
378 $Ar_3PO^{\bullet+}$ (path h). Finally, the last intermediate reacted with
379 superoxide ion, giving another molecule of Ar_3PO and molecular
380 oxygen (path i).

381 An active role of singlet oxygen that is formed during the
382 oxidative photoreaction was excluded because the reaction between
383 $Ar_3P^{\bullet+}$ and molecular oxygen is faster than expected. In fact,
384 comparison of the bimolecular rate constant between Ph_3P and
385 singlet oxygen ($k_r = 1.6 \times 10^7 M^{-1} s^{-1}$)²³ and the bimolecular rate
386 constant between $Ph_3P^{\bullet+}$ and molecular oxygen ($k_2 = 1.6 \times$
387 $10^{10} M^{-1} s^{-1}$ for DCA/biphenyl, and $k_2 = 3.4 \times 10^{10} M^{-1} s^{-1}$ for
388 NMQ^+ in MeCN)^{22e} makes it clear that singlet oxygen sensi-
389 tization cannot compete efficiently with path g (see Scheme 8).
390 Furthermore, formation of intermediate $Ar_3PO_2^{\bullet+}$ was proposed
391 for path g instead of a phosphodioxirane intermediate (Ph_3PO_2),²³
392 as recently demonstrated in the photosensitized electron-transfer
393 oxidation of triphenylphosphine with DCA and NMQ^+ in differ-
394 ent organic solvents.^{22e} Therefore, we excluded the reaction of
395 singlet oxygen with arylphosphines from the reaction mechanism
396 as a competitive oxidative pathway.

397 As mentioned for the co-oxidation of sulfides, superoxide ion is
398 not involved in the oxidation pathway and coupling of $Ph_3P^{\bullet+}$
399 with superoxide ion has been excluded. Therefore, the role of
400 $O_2^{\bullet-}$ is to operate as an electron carrier in the reduction of
401 intermediate $Ph_3PO^{\bullet+}$, as depicted in path i (see Scheme 8).

402 We can conclude that two competitive oxidation pathways
403 exist, oxygen transfer from intermediates I and III to Ar_3P (paths
404 b and c, respectively) and subsequent oxidation of triarylphos-
405 phine radical cation (paths h and i). However, intermediates I
406 and III arise from the electrocyclization of $1^{\bullet+}$ with a rate con-
407 stant that is lower than the rate constant of the electron-transfer
408 process between $1^{\bullet+}$ and Ar_3P . Therefore, the last competitive
409 pathway prevails significantly over the first oxidation pathway
410 because inhibition of the consumption of amine 1 in the presence
411 of Ar_3P was clearly described.

412 CONCLUSIONS

413 The photochemical co-oxidation of sulfides and phosphines
414 examined in this paper takes place through at least two distinct
415 reaction mechanisms, depending on the nucleophilicity of the
416 substrates used. In any case, irradiation of tris(*p*-bromophenyl)-
417 amine (1) gives the corresponding radical cation $1^{\bullet+}$. The inter-
418 mediate can undergo electrocyclization to 2 that in turn reacts
419 with molecular oxygen to provide peroxy I and hydroperoxy II
420 radicals, successively. These last two intermediates are potential
421 oxidants and react with a mechanism that depends on the sub-
422 strate used. Thus, sulfides are oxidized by hydroperoxy II, while
423 phosphines are oxidized by peroxy I because of the strong nucle-
424 ophilicity of these substrates in comparison with that of sulfides.
425 In addition, consumption of amine 1 is observed in the presence
426 of sulfides but in the presence of phosphines is significantly
427 inhibited. On the other hand, for the case of *p*-methoxythioani-
428 sole and triarylphosphines, a one-electron-transfer process
429 between $1^{\bullet+}$ and these substrates operates efficiently (path f in
430 both Schemes 7 and 8), which is supported by laser flash
431 photolysis experiments. Then, reaction of *p*-methoxythioanisole
432 and triarylphosphine radical cations with molecular oxygen gave

intermediates R_2SOO^{*+} and Ar_3POO^{*+} , respectively, that finally were converted into the corresponding oxides (path h in Scheme 5 for sulfides and paths h and i in Scheme 8 for phosphines). Singlet oxygen sensitization of sulfides and phosphines was excluded from the reaction mechanism as a competitive oxidation pathway because reaction of triarylphosphine radical cation with molecular oxygen is faster than singlet oxygen sensitization (compare the rate constant of singlet oxygen, $k = 1.6 \times 10^7 \text{ M}^{-1} \text{ s}^{-1}$, with the rate constant of Ph_3P^{*+} with molecular oxygen, $k = 1.6 \times 10^{10} \text{ M}^{-1} \text{ s}^{-1}$) and the product distributions obtained for sulfides under our experimental conditions are not those expected for a singlet oxygen sensitization. In fact, under singlet oxygen sensitization, Ph_2S is unreactive with respect to singlet oxygen while benzyl ethyl sulfide gives benzaldehyde and the corresponding sulfoxide and sulfone.^{14a,b} Furthermore, thioanisole and *p*-methoxythioanisole give the corresponding sulfoxides and sulfones as the main products under singlet oxygen sensitization.^{14c} Finally, the role of superoxide ion that is formed during irradiation of **1** under an oxygen atmosphere operates as an electron carrier that is involved for sulfides in path h (see Schemes 6 and 7) and for phosphines in path i (see Scheme 8) and does not react directly with sulfides and phosphine radical cations, respectively.^{19,22e} In conclusion, the photoionization of the Magic Blue precursor (amine **1**) is a versatile tool for promoting oxidation of organic substrates.

EXPERIMENTAL DETAILS

Materials. Tris(*p*-bromophenyl)amine, thioanisole, *p*-methoxythioanisole, diphenyl sulfide, triphenylphosphine, triphenylphosphine oxide, tris(2-methylphenyl)phosphine, tris(2,4,6-trimethylphenyl)phosphine, diphenyl sulfoxide, methyl phenyl sulfoxide, *p*-methoxyphenyl methyl sulfoxide, benzaldehyde, and benzophenone were commercial products. Sulfoxides and triarylphosphine oxides used as reference compounds were prepared by reported procedures.²⁴ The benzyl ethyl sulfide²⁵ and the corresponding sulfoxide²⁶ were prepared by reported procedures.

Co-Oxidation Reactions. The co-oxidation experiments were performed by using $5.0 \times 10^{-3} \text{ M}$ **1** in the presence of 0.01 M solutions of the chosen sulfide or triarylphosphine in different solvents (2,2,2-trifluoroethanol, acetonitrile, acetonitrile/water mixture, and dichloromethane). The solutions were contained in rubber-stoppered, 1 cm diameter quartz tubes, and a stream of dry oxygen saturated with the appropriate solvent was passed into the solution through a needle for 10 min in the dark. The quartz tubes were exposed to 10 phosphor-coated 15 W lamps (Rayonet) emitting at 366 nm. The products were assessed by GC on the basis of calibration curves in the presence of cyclododecane as the internal standard.

Time-Resolved Laser Flash Spectroscopy. Nanosecond-to-microsecond transient absorption experiments were performed using a nanosecond laser flash photolysis apparatus equipped with a 20 Hz Nd:YAG laser (20 ns, 1 mJ at 355 and 266 nm) and a 150 W Xe flash lamp as the probe light. Samples were placed in a quartz cell (10 mm \times 10 mm section) at a concentration adjusted to obtain an OD value of 1.0 at 355 nm. Nonlinear fitting procedures by the least-squares method and χ^2 and the distribution of residuals were used to judge the goodness of fit. Quantum yields of formation [ϕ (see Table 1)] for **1**^{•+} and **2** were measured by comparison of the zero time intensity of the signal of the transients with that of the ketyl radical formed after flash excitation (355 nm) of a solution (in benzene) of benzophenone.

ASSOCIATED CONTENT

Supporting Information

The Supporting Information is available free of charge on the ACS Publications website at DOI: 10.1021/acs.joc.8b00913.

Determination of the kinetic data of transient decay traces, determination of the rate data of product formation,

¹H NMR and ¹³C NMR spectra of compound **1**, and ¹H spectra of compound **1** irradiated in MeCN (reaction mixture) (PDF)

AUTHOR INFORMATION

Corresponding Author

*E-mail: smbonesi@qo.fcen.uba.ar. Phone and fax: +541145763346.

ORCID

Sergio M. Bonesi: 0000-0003-0722-339X

Stefano Protti: 0000-0002-5313-5692

Notes

The authors declare no competing financial interest.

ACKNOWLEDGMENTS

S.M.B. is a research member of CONICET (Argentinean National Research Council).

REFERENCES

- (1) Plesniak, M. P.; Huang, H.-M.; Procter, D. J. Radical cascade reactions triggered by single electron transfer. *Nature Rev. Chem.* **2017**, *1*, 0077.
- (2) (a) Lligadas, G.; Grama, S.; Percec, V. Single-Electron Transfer Living Radical Polymerization Platform to Practice, Develop, and Invent. *Biomacromolecules* **2017**, *18*, 2981–3008. (b) Zhang, N.; Samanta, S. R.; Rosen, B. M.; Percec, V. Single Electron Transfer in Radical Ion and Radical-Mediated Organic, Materials and Polymer Synthesis. *Chem. Rev.* **2014**, *114*, 5848–5958. (c) Branchini, B. R.; Behney, C. E.; Southworth, T. L.; Fontaine, D. M.; Gulick, A. M.; Vinyard, D. J.; Brudvig, G. W. Experimental Support for a Single Electron-Transfer Oxidation Mechanism in Firefly Bioluminescence. *J. Am. Chem. Soc.* **2015**, *137*, 7592–7595.
- (3) (a) Creutz, S. E.; Lotito, k. J.; Fu, G. C.; Peters, J. C. Photoinduced Ullmann C–N Coupling: Demonstrating the Viability of a Radical Pathway. *Science* **2012**, *338* (6107), 647–651. (b) Quiroz-Guzman, M.; Brown, S. N. Tris(4-bromo-phenyl)aminium hexachloroantimonate (Magic Blue[®]): a strong oxidant with low inner-sphere reorganization. *Acta Crystallogr., Sect. C: Cryst. Struct. Commun.* **2010**, *66*, m171–m173.
- (4) (a) Breslin, D. T.; Fox, M. A. Photochemical Electrocyclization of Thermally Stable Triarylamine Radical Cations. *J. Org. Chem.* **1994**, *59*, 7557–7561. (b) Breslin, D. T.; Fox, M. A. Excited-State Behavior of Thermally Stable Radical Ions. *J. Phys. Chem.* **1994**, *98*, 408–411.
- (5) (a) Yurchenko, O.; Freytag, D.; zur Borg, L.; Zentel, R.; Heinze, J.; Ludwigs, S. Electrochemically Induced Reversible and Irreversible Coupling of Triarylaminines. *J. Phys. Chem. B* **2012**, *116*, 30–39. (b) Baranoff, E.; Dixon, I. M.; Collin, J. P.; Sauvage, J. P.; Ventura, B.; Flamigni, L. Dyads Containing Iridium(III) Bis-terpyridine as Photoactive Center: Synthesis and Electron Transfer Study. *Inorg. Chem.* **2004**, *43*, 3057–3066. (c) Flamigni, L.; Baranoff, E.; Collin, J. P.; Sauvage, J. P. A Triad Based on an Iridium(III) Bisterpyridine Complex Leading to a Charge-Separated State with a 120- μ s Lifetime at Room Temperature. *Chem. - Eur. J.* **2006**, *12*, 6592–6606.
- (6) Bonesi, S. M.; Dondi, D.; Protti, S.; Fagnoni, M.; Albin, A. (Co)oxidation/cyclization processes upon irradiation of triphenylamine. *Tetrahedron Lett.* **2014**, *55*, 2932–2935.
- (7) Wilkinson, F.; Abdel-Shafi, A. A. Mechanism of Quenching of Triplet States by Oxygen: Biphenyl Derivatives in Acetonitrile. *J. Phys. Chem. A* **1997**, *101*, 5509–5516.
- (8) (a) Silva, E. F. F.; Serpa, C.; Dabrowski, J. M.; Monteiro, C. J. P.; Formosinho, S. J.; Stochel, G.; Urbanska, K.; Simões, S.; Pereira, M. M.; Arnaut, L. G. Mechanisms of Singlet-Oxygen and Superoxide-Ion Generation by Porphyrins and Bacteriochlorins and their Implications in Photodynamic Therapy. *Chem. - Eur. J.* **2010**, *16*, 9273–9286. (b) Abdel-Shafi, A. A.; Wilkinson, F. Electronic to vibrational energy conversion and charge transfer contributions during quenching of molecular oxygen of electronically excited triplet states. *Phys. Chem.*

- 559 *Chem. Phys.* **2002**, *4*, 248–254. (c) Abdel-Shafi, A. A.; Wilkinson, F.
560 Charge Transfer Effects on the Efficiency of Singlet Oxygen Production
561 Following Oxygen Quenching of Excited Singlet and Triplet States of
562 Aromatic Hydrocarbons in Acetonitrile. *J. Phys. Chem. A* **2000**, *104*,
563 5747–5757.
- 564 (9) Liang, J. J.; Gu, C. L.; Kacher, M. L.; Foote, C. S. Chemistry of
565 singlet oxygen. 45. Mechanism of the photooxidation of sulfides. *J. Am.*
566 *Chem. Soc.* **1983**, *105*, 4717–4721.
- 567 (10) Parisien-Collette, S.; Hernández-Pérez, A. C.; Collins, Sh. K
568 Photochemical Synthesis of Carbazoles Using an $[\text{Fe}(\text{phen})_3](\text{NTf}_2)_2$ /
569 O_2 Catalyst System: Catalysis toward Sustainability. *Org. Lett.* **2016**, *18*,
570 4994–4997.
- 571 (11) (a) Amthor, S.; Noller, B.; Lambert, C. UV/Vis/NIR spectral
572 properties of triaryl amines and their corresponding radical cations.
573 *Chem. Phys.* **2005**, *316*, 141–152. (b) Ambrose, J. F.; Carpenter, L. L.;
574 Nelson, R. F. Electrochemical and Spectroscopic Properties of Cation
575 Radicals III. Reaction Pathways of Carbazolium Radical Ions. *J.*
576 *Electrochem. Soc.* **1975**, *122*, 876–894. (c) Cho, S. H.; Yoon, J.;
577 Chang, S. Intramolecular Oxidative C–N Bond Formation for the
578 Synthesis of Carbazoles: Comparison of Reactivity between the Copper-
579 Catalyzed and Metal-Free Conditions. *J. Am. Chem. Soc.* **2011**, *133*,
580 5996–6005. (d) Jordan-Hore, J. A.; Johansson, C. C. C.; Gulias, M.;
581 Beck, E. M.; Gaunt, M. J. Oxidative Pd(II)-Catalyzed C–H Bond
582 Amination to Carbazole at Ambient Temperature. *J. Am. Chem. Soc.*
583 **2008**, *130*, 16184–16186. (e) Sridharan, V.; Martin, M. A.; Menéndez, J.
584 C. Synthesis of Oxygenated Carbazoles by Palladium-Mediated
585 Oxidative Double C–H Activation of Diarylamines Assisted by
586 Microwave Irradiation. *Synlett* **2006**, *2006*, 2375–2378. (f) Hernán-
587 dez-Pérez, A. C.; Collins, S. K. A visible-light-mediated synthesis of
588 carbazoles. *Angew. Chem., Int. Ed.* **2013**, *52*, 12696–12700. (g) Hernán-
589 dez-Pérez, A. C.; Caron, A.; Collins, S. K. Photochemical Synthesis of
590 Complex Carbazoles: Evaluation of Electronic Effects in Both UV- and
591 Visible-Light Methods in Continuous Flow. *Chem. - Eur. J.* **2015**, *21*,
592 16673–16678. (h) Bedford, R. B.; Betham, M. N-H Carbazole Synthesis
593 from 2-Chloroanilines via Consecutive Amination and C–H Activation.
594 *J. Org. Chem.* **2006**, *71*, 9403–9410. (i) Bedford, R. B.; Cazin, C. S. J. A
595 novel catalytic one-pot synthesis of carbazoles via consecutive amination
596 and C–H activation. *Chem. Commun.* **2002**, 2310–3211.
- 597 (12) Buxton, G. V.; Greenstock, C. L.; Helman, W. P.; Ross, A. B.
598 Critical Review of rate constants for reactions of hydrated electrons,
599 hydrogen atoms and hydroxyl radicals ($\cdot\text{OH}/\cdot\text{O}^-$ in Aqueous Solution.
600 *J. Phys. Chem. Ref. Data* **1988**, *17*, 513.
- 601 (13) (a) Janata, E. Direct optical observation of the formation of some
602 aliphatic alcohol radicals. A pulse radiolysis study. *Proc. - Indian Acad.*
603 *Sci., Chem. Sci.* **2002**, *114*, 731–737. (b) Hare, P. M.; Price, E. A.;
604 Stanisky, Ch. M.; Janik, I.; Bartels, D. M. Solvated Electron Extinction
605 Coefficient and Oscillator Strength in High Temperature Water. *J. Phys.*
606 *Chem. A* **2010**, *114*, 1766–1775. (c) Lemmon, R. M.; Pohlit, H. M.;
607 Erwin, W.; Lin, T.-H. Hot-atom chemistry of carbon-14 in solid benzene
608 at kinetic energies between 5 and 100 eV. *J. Phys. Chem.* **1971**, *75*, 2555–
609 2557. (d) Wolfenden, B. S.; Willson, R. L. Radical-cations as reference
610 chromogens in kinetic studies of one-electron transfer reactions: pulse
611 radiolysis studies of 2,2'-azinobis-(3-ethylbenzthiazoline-6-sulphonate).
612 *J. Chem. Soc., Perkin Trans. 2* **1982**, 805–812. (e) Wala, M.; Bothe, E.;
613 Goerner, H.; Schulte-Frohlinde, D. Quantum yields for the generation
614 of hydrated electrons and single-strand breaks in poly(C), poly(A) and
615 single-stranded DNA in aqueous solution on 20 ns laser excitation at 248
616 nm. *J. Photochem. Photobiol., A* **1990**, *53*, 87–108.
- 617 (14) (a) Bonesi, S. M.; Mella, M.; d'Alessandro, N.; Aloisi, A.; Vanossi,
618 M.; Albini, A. Photosensitized oxygenation of benzyl ethyl sulfide. *J. Org.*
619 *Chem.* **1998**, *63*, 9946–9955. (b) Bonesi, S. M.; Torriani, R.; Mella, M.;
620 Albini, A. The photooxygenation of benzyl, heteroarylmethyl and allyl
621 sulfides. *Eur. J. Org. Chem.* **1999**, *1999*, 1723–1728. (c) Bonesi, S. M.;
622 Fagnoni, M.; Albini, A. Hammett correlations in the photosensitized
623 oxidation of 4-substituted thioanisoles. *J. Org. Chem.* **2004**, *69*, 928–935.
624 (d) Clennan, E. L. Persulfoxide: Key Intermediate in Reactions of
625 Singlet Oxygen with Sulfides. *Acc. Chem. Res.* **2001**, *34*, 875–884.
- (15) Hermans, I.; Peeters, J.; Jacobs, P. A. Autoxidation of
Hydrocarbons: From Chemistry to Catalysis. *Top. Catal.* **2008**, *50*,
124–132.
- (16) Reynolds, R.; Line, L. L.; Nelson, R. F. Electrochemical generation
of carbazoles from aromatic amines. *J. Am. Chem. Soc.* **1974**, *96*, 1087–
1092.
- (17) Goto, Y.; Matsui, T.; Ozaki, S.; Watanabe, Y.; Fukuzumi, Sh
Mechanisms of Sulfoxidation Catalyzed by High-Valent Intermediates
of Heme Enzymes: Electron-Transfer vs Oxygen-Transfer Mechanism.
J. Am. Chem. Soc. **1999**, *121*, 9497–9502.
- (18) Baciocchi, E.; Del Giacco, T.; Elisei, F.; Gerini, M. F.; Guerra, M.;
Lapi, A.; Liberali, P. Electron Transfer and Singlet Oxygen Mechanisms
in the Photooxygenation of Dibutyl Sulfide and Thioanisole in MeCN
Sensitized by N-Methylquinolinium Tetrafluoroborate and 9,10-Dicya-
noanthracene. The Probable Involvement of a Thiadioxirane Inter-
mediate in Electron Transfer Photooxygenations. *J. Am. Chem. Soc.*
2003, *125*, 16444–16454.
- (19) Bonesi, S. M.; Manet, I.; Freccero, M.; Fagnoni, M.; Albini, A.
Photosensitized oxidation of Sulfides: Discriminating between the
Singlet-Oxygen Mechanism and Electron Transfer Involving Superoxide
Anion or Molecular Oxygen. *Chem. - Eur. J.* **2006**, *12*, 4844–4857.
- (20) Nakamura, M.; Miki, M.; Majima, T. Substituent effect on the
photoinduced electron-transfer reaction of para-substituted triphenyl
phosphines sensitised by 9,10-dicyanoanthracene. *J. Chem. Soc., Perkin*
Trans. **2000**, *2*, 1447–1452.
- (21) (a) Lalevée, J.; Allonas, X.; Fouassier, J. P. New access to the
peroxyl radicals reactivity? *Chem. Phys. Lett.* **2007**, *445*, 62–67.
(b) Fukuzumi, S.; Shimoosako, K.; Suenobu, T.; Watanabe, Y.
Mechanisms of Hydrogen-, Oxygen-, and Electron-Transfer Reactions
of Cumylperoxyl Radical. *J. Am. Chem. Soc.* **2003**, *125*, 9074–9082.
- (22) (a) Yasui, S.; Rahman Badal, M.; Kobayashi, S.; Mishima, M.
Combination of LFP-TRIR spectroscopy and DFT computation as a
tool to determine the intermediate during the photooxidation of
triphenylphosphine. *J. Phys. Org. Chem.* **2014**, *27*, 967–972. (b) Yasui, S.;
Rahman Badal, M.; Kobayashi, S.; Mishima, M. Kinetic study of
photoreaction of triarylphosphines by laser flash photolysis time-
resolved UV-VIS spectroscopy. *Chem. Lett.* **2013**, *42*, 866–868.
(c) Ohkubo, K.; Nanjo, T.; Fukuzumi, S. Photocatalytic Electron-
Transfer Oxidation of Triphenylphosphine and Benzylamine with
Molecular Oxygen via Formation of Radical Cations and Superoxide
Ion. *Bull. Chem. Soc. Jpn.* **2006**, *79*, 1489–1500. (d) Beaver, B.; Rawlings,
D.; Neta, P.; Alfassi, Z. B.; Das, T. N. Structural effects on the reactivity
of substituted arylphosphines as potential oxygen-scavenging additives
for future jet fuels. *Heteroat. Chem.* **1998**, *9*, 133–138. (e) Bonesi, S. M.;
Protti, S.; Albini, A. Reactive Oxygen Species (ROS)-vs Peroxyl-
Mediated Photosensitized Oxidation of Triphenylphosphine: A
Comparative Study. *J. Org. Chem.* **2016**, *81*, 11678–11685.
- (23) Zhang, D.; Ye, B.; Ho, D. G.; Gao, R.; Selke, M. Chemistry of
singlet oxygen with arylphosphines. *Tetrahedron* **2006**, *62*, 10729–
10733.
- (24) (a) Bordwell, F. G.; Boutan, P. Synthesis of Aryl Methyl
Sulfoxides and Determination of the Conjugative Effect of the
Methylsulfinyl Group. *J. Am. Chem. Soc.* **1957**, *79*, 717–722. (b) Seneor,
A. E.; Valient, W.; Wirth, J. Derivatives of Triphenylphosphine and
Triphenylphosphine Oxide. *J. Org. Chem.* **1960**, *25*, 2001–2006.
- (25) Modena, G.; Taddei, F.; Todesco, P. E. Nucleophilic substitutions
in ethylene derivatives: 1-arylsulfonyl-1-methyl-2-haloethylenes. *Gazz.*
Chim. Ital. **1960**, *89*, 894.
- (26) Cerniani, A.; Modena, G.; Todesco, P. E. Oxidation of organic
sulfides. IV. Oxidation of benzyl and phenyl alkyl sulfoxides to sulfones.
Gazz. Chim. Ital. **1960**, *90*, 3.